

## **PULLOUT CAPACITY OF BLOCK ANCHOR IN UNSATURATED SAND**

Naser Al-Shayea<sup>1</sup>

<sup>1</sup> *Civil Engineering Department, KFUPM, Box 368, Dhahran 31261, Saudi Arabia;*  
PH (966 3) 860-2480; FAX (966 3) 860-2879; e mail: nshayea@kfupm.edu.sa

### **ABSTRACT**

Block anchor is an interface element used to restrain horizontal movement of structures. This paper investigates the effect of moisture conditions (or degree of saturation) on the pullout capacity of block anchor embedded in sand at three different moisture conditions. The approach taken consists of experimental work, and analytical calculation. The experimental work is pullout tests, made in the laboratory, on 0.15 x 0.15 x 0.15m concrete block anchors embedded in sand, at a depth of 0.15m. The sand is deposited in a 1.2 x 0.6 x 0.8m box using a pluviation method to ensure a uniform and reproducible density. Materials used were characterized to find their properties, and the equipments used were calibrated before usage. The load and the corresponding horizontal and vertical displacements were recorded. In addition, visual observations were made on the failed soil body. The experimental results are compared with the analytical calculations (by Rankine, Coulomb, and log spiral theories). The 3-D effect was also considered.

The block anchor was found to have higher pullout capacity than a plate anchor. The results show that the moisture condition significantly affects the pullout capacity of the block anchor. The pullout capacity of the block anchor embedded in unsaturated (wet) sand is about double that for the block embedded in dry sand, while that for the block embedded in saturated sand is only about one half of that for the block embedded in dry sand. These findings have very significant implications in the analysis and design of the block anchor embedded in unsaturated sand. Also, these have contributions to the hazard risk assessment of block anchors embedded in sand subjected to variations in degree of saturation.

### **1. INTRODUCTION**

Lateral earth pressure is a significant parameter in soil-structure-interaction problems involving underground substructures embedded in the soil body, such as

anchors. Anchors are interface elements between the ground and structures, and are used to stabilize earth structures by constraining displacement or movement. They transfer forces in a given direction from the structure to the ground (soil or rock). Anchor types include: anchor plates and beams (deadman), tie backs, vertical anchors, anchor beams supported by batter piles, and block anchors. Block anchor is a cast-in-place or pre-cast concrete member that may be square or rectangular in section with the necessary length to develop adequate passive resistance, Bowles (1997). They are specially designed to withstand pullout or thrust forces.

Review of literature reveals that many research studies have been conducted on the capacity of vertical anchor. Many studies were found to study anchor plate, including Hueckel (1957), Ovesen and Stromann (1972), Neely, et al. (1973), Das (1975), Akinmusuru (1978), Dickin and Leung (1983), and Ghaly (1997). But only few studies were found for block anchor, Bowles (1997) and Duncan and Mokwa (2001). Eleven researches were lab experimental works, one was a review work, and one was field experimental work.

This paper investigates the pullout capacity of block anchors embedded in sand using small scale laboratory models, with three different moisture conditions of the soil (dry, saturated, and saturated-then-gravity-drained). Experimental results are compared with those from analytical analyses.

## 2. THEORETICAL ANALYSIS

### 2.1 Theories of lateral earth pressure

There are three well-known analytical theories dealing with the passive earth pressures, namely: Rankine theory (smooth structure), Coulomb theory (rough structure), and Log spiral theory (curved failure surface). The theoretical value of lateral earth pressure is dependent on the theories used and on the assumptions made relative to the nature of the structure, the soil, and the soil-structure interface.

### 2.2. Forces acting on anchor block

Figure 1 shows a cross section of a short anchor block embedded in sand, with all forces acting on it and with friction considered. For an anchor block with the dimensions: width (B), depth (h), thickness (t), depth of embedment below soil surface (d), and the distance from the upper edge of the anchor to the pulling load (z); the forces are as follows:

$P_u$  = ultimate pullout capacity of the block anchor embedded in sand,

$P_p$  = effective passive force =  $K_p * \gamma * (d+h/2) * h * B$ ,

$P_a$  = effective active force of soil =  $K_a * \gamma * (d+h/2) * h * B$ ,

$F_t$  = effective friction force at the top of the block =  $W_s * \tan \delta_b$ ,

$F_b$  = effective friction force at the bottom of the block =  $N * \tan \delta_b$ ,

$F_s$  = effective friction force at two sides of the block =  $2 * K_o * \gamma * (d+h/2) \tan \delta_s * h * t$ ,

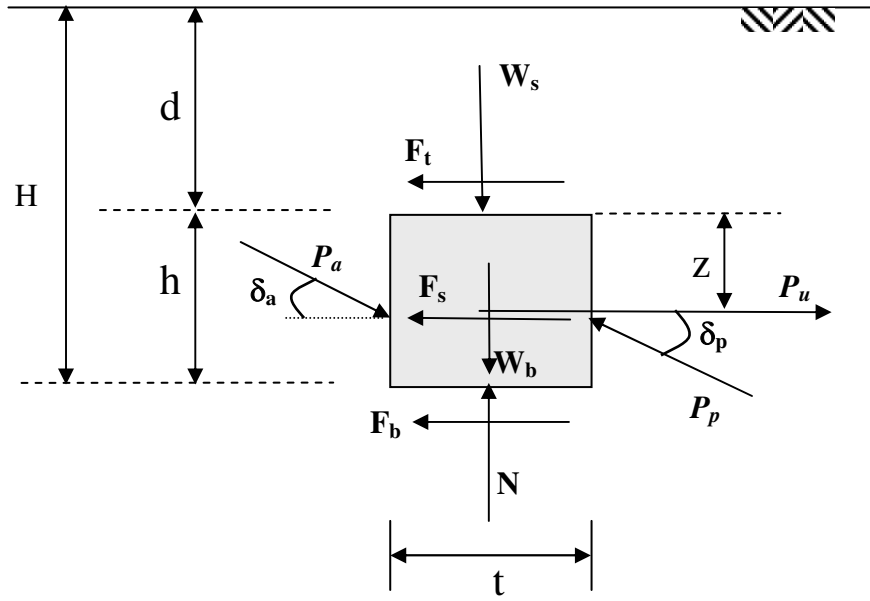


**Figure 1. Block anchor with acting forces.**

$W_s$  = weight of soil above the block anchor =  $\gamma' * d * t * B$ ,

$W_b$  = weight of the block anchor =  $\gamma'_c * h * t * B$ , and

$N$  = normal force.

Where:  $\gamma'$  = effective unit weight of the soil,

$\gamma'_c$  = effective unit weight of concrete,

$K_p$  = coefficient of passive lateral earth pressure,

$K_a$  = coefficient of active lateral earth pressure,

$K_o$  = coefficient of lateral earth pressure at rest,

$\delta_t$  = angle of friction between soil and top surface of the block, and

$\delta_b$  = angle of friction between soil and bottom surface of the block.

The passive and active forces ( $P_p$  and  $P_a$ ) are inclined by  $\delta_p$  and  $\delta_a$ , respectively to the normal-to-the-surface of the block side, where,  $\delta_p$  is the angle of friction between soil and passive side surface of the block, and  $\delta_a$  is the angle of friction between soil and active side surface of the block. The horizontal components of the passive and active forces ( $P_{p,h}$  and  $P_{a,h}$ ) are:  $P_{p,h} = P_p * \cos \delta_p$ , and  $P_{a,h} = P_a * \cos \delta_a$ .

The vertical components of the passive and active forces ( $P_{p,v}$  and  $P_{a,v}$ ) are the effective friction forces ( $F_p$  and  $F_a$ ) at the passive and active side surfaces of the block anchor, respectively, and they are:  $P_{p,v} = P_p * \sin \delta_p$ , and  $P_{a,v} = P_a * \sin \delta_a$ .

### 2.3. Friction between Soil and Structure ( $\delta$ )

Coulomb's theory considers friction between the soil and the structure. Notice that this friction is between the soil and the vertical sides of the structure. The

angle of friction between soil and structure is  $\delta$ . Considering the  $\delta$ -value, Coulomb's theory gives a higher value of passive pressure and a lower value of active pressure as compared to Rankine's theory, which likely produces overestimation (conservative), Bowles (1997).

As an approximation, Singh (1967) suggested the following values for  $\delta$ : (1)  $\delta = 1/3 \bar{\phi}$  for smooth structure (wall), (2)  $\delta = 2/3 \bar{\phi}$  for ordinary retaining wall, (3)  $\delta = 3/4 \bar{\phi}$  for rough walls with well-drained backfill, and (4)  $\delta = 0$  when the backfill is subjected to vibrations, where  $\bar{\phi}$  is the effective angle of internal friction of the soil. The range of values of  $\delta$  between fine sand and concrete is 15-25°, Bowles (1997) and Das (1995). All values of  $\delta$  suggested above are for the maximum value ( $\delta_{max}$ ).

The actual value is the mobilized friction angle ( $\delta_{mobilized}$ ), which is less than the corresponding maximum value. The value of  $\delta_{mobilized}$  is governed by the following factors:

- Maximum possible value of the friction ( $\delta_{max}$ ), which depends on the roughness of the interface and the properties of the soil.
- Relative shear displacement along the interface; which mobilize the interface friction.
- Vertical equilibrium of the forces acting on the structure.
- Weight of the anchor (light vs. heavy).

The angles for the horizontal friction  $\delta_t$  and  $\delta_b$  are taken to be equal to  $\delta_{max}$ , and the angles for the vertical friction  $\delta_p$  and  $\delta_a$  are taken to be equal to  $\delta_{mobilized}$ . Notice that Ovesen and Stromann (1972) considered  $\delta_a$  to be equal to the angle of internal friction of the soil ( $\phi$ ).

The mobilized friction angle ( $\delta_{mobilized}$ ) can be found from the equilibrium of forces acting on the block shown in Figure 1. For light-weight anchor, the vertical components of the passive and active forces ( $P_{p,v} - P_{a,v}$ ) is greater than the weight of the block and the soil above it ( $W_b + W_s$ ), and therefore slip does not occur on the interface between the block and the soil. This condition causes uplift of the anchor, making the normal force ( $N$ ) equals zero. By summing forces along the vertical direction, with  $N = 0$ , yields:

$$\delta_{mobilized} = \sin^{-1} \left( \frac{W_b + W_s}{P_p - P_a} \right) \quad (1)$$

#### 2.4. 3-D Effect

Based on the shape of the anchor, there are two types: long/continuous (plane strain, 2-D problem) and short (3-D problem). Theories of lateral earth pressures (Rankine, Coulomb, and Log spiral) were developed for 2-D situation. The

conditions at the ends of the structure are quite different from those at the center, which have significant influence on the passive resistance. Ovesen (1964) found that the passive earth pressure against short structures is higher than those predicted by conventional theories (Rankine and Coulomb theories), and the difference can be quite significant. Hansen (1966) developed a method for correcting the results of conventional pressure theories for shape (or 3-D) effects. For short anchors, the ultimate resistance should be multiplied by a correction factor (M) to account for 3-D effects. For a plate anchor, M is given as:

$$M = 1 + (K_p - K_a)^{0.67} \left[ 1.1E^4 + \frac{1.6F}{1 + 5(B/h)} + \frac{0.4(K_p - K_a)E^3 F^2}{1 + 0.05(B/h)} \right] \quad (2)$$

where,  $E = 1 - h/(d+h)$ ,

$F = 1 - (B/S)^2$ , and

$S =$  center-to-center distance between two anchors.

The above equation considers both the embedment factor (E) and the shape factor (F). The value of E is 0.5 for  $d = h$ . The value of F is 0.0 for long/continuous anchor, and is 1.0 for single short anchor.

## 2.5. Capacity of Block Anchor

The ultimate capacity of block anchor ( $P_u$ ) can be found from the equilibrium of forces acting on the block shown in Figure 1. By summing forces along the horizontal direction and multiplying the lateral earth pressure (passive and active) by the 3-D correction factor (M) given in Equation (2), yields:

$$P_u = M(P_{p,h} - P_{a,h}) + F_t + F_s + F_b \quad (3)$$

For Coulomb and Log spiral theories,  $F_b = 0$  (as  $N = 0$ ). The allowable capacity of block anchor is  $P_{all} = P_u / FS$ , where,  $FS$  is a factor of safety of 1.2 to 1.5, as suggested by Bowles (1997).

## 3. EXPERIMENTAL INVESTIGATION

### 3.1. Material Characterization

#### 3.1.1 Soil

The sand used in this research was selected to be the fraction of beach sand that passes sieve #30 and is retained in sieve #100. Various tests were made to characterize this sand according to the respective ASTM Standards. The grain size distribution curve of this sand indicated that  $D_{10}$ ,  $D_{30}$ , and  $D_{60}$  are 0.18mm, 0.29mm, and 0.38mm, respectively. The coefficient of uniformity ( $C_u$ ) equals 2.11, and the coefficient of concavity/curvature ( $C_z$ ) equals 1.23. According to Unified Soil Classification System (USCS), this sand is categorized as poorly-graded clean sand

(SP). This sand has a specific gravity ( $G_s$ ) of 2.679, and maximum and minimum densities of  $1889.58 \text{ kg/m}^3$  and  $1662.78 \text{ kg/m}^3$ , respectively.

This research used pluviation method to produce uniformly dense, homogenous, isotropic, and reproducible sand deposits in the sand box. The optimum height of fall was found to be 100 cm. This height of fall was subsequently used to fill the box with sand for the pullout tests. The corresponding dry density is  $1774 \text{ kg/m}^3$ , i.e. the dry unit weight ( $\gamma_d$ ) is  $17.398 \text{ kN/m}^3$ . This gives a relative density ( $D_r$ ) of 60.3%; i.e., medium density. Using phase relationships, the void ratio ( $e$ ) is 0.51, and the saturated unit weight ( $\gamma_{\text{sat}}$ ) is  $20.711 \text{ kN/m}^3$ .

The above dry density was used for permeability and strength tests, as well as for analytical computations. The coefficient of permeability, at that was found to be  $0.01476 \text{ cm/s}$  ( $1.476 \times 10^{-4} \text{ m/sec}$ ); i.e., within the range of medium permeability of fine sand.

Both direct shear tests and triaxial shear tests were performed to determine the angle of internal friction ( $\phi$ ) of this cohesionless sand. Direct shear tests were performed on dry sand at four different of normal loads; 20 kgf (196.1 N), 40 kgf (392.3 N), 80 kgf (784.5 N), and 160 kgf (1569.6 N). The resulted angle of internal friction ( $\phi$ ) is  $44.9^\circ$ . Three sets of drained CD triaxial tests were performed on sand at three different moisture conditions; dry, wet, and saturated. Tests were made at confining pressures ( $\sigma_c$ ) of 25, 50, 100, and 200 kPa, so low to resemble those at shallow depths. A cycle of unloading and reloading was made for each test. Figure 2 shows typical plots for the deviator stress versus the axial strain for dry, wet, and saturation conditions of sand. The resulted angle of internal friction ( $\phi$ ) is  $43.5^\circ$ , a little lower than that from the direct shear test. For wet condition, the resulted apparent cohesion is about  $17 \text{ kN/m}^2$ , which is attributed to capillarity effects.

To assess the stiffness of the sand at shallow depths; the initial modulus ( $E_0$ ), the secant modulus ( $E_{50}$ ), and the dilatancy angle ( $\psi$ ) were obtained from the results of triaxial tests at low confining pressure, and tabulated in Table 1. At a given confining pressure, the moduli are largest at wet condition, and smallest at saturated condition; while the dilatancy angle is largest at dry condition, and smallest at wet condition.

### *3.1.2 Friction between Soil and Concrete*

Maximum friction angle between soil and concrete and between soil and steel were determined using the direct shear apparatus. Concrete or steel specimen having a dimension of 6 cm length, 6 cm width, and 1 cm thickness was placed in lower half of shear box, and sand at density of  $1774 \text{ kg/m}^3$  was placed at the upper half. The angle of friction between soil and concrete were found to be  $38.0^\circ$ . The angle of friction between soil and steel were found to have an average value of  $28.7^\circ$ . This represents the value for  $\delta_{\text{max}}$ .

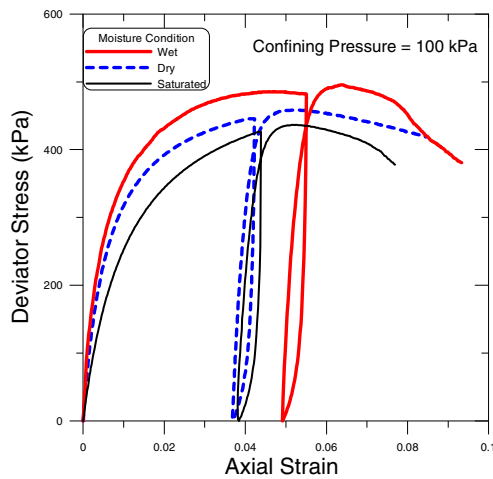


**Figure 2. Results of triaxial tests on sand, under a confining pressure of 100 kPa, at dry, wet, and saturation conditions.**

**Table 1 Moduli of Elasticity and Dilatancy Angle**

Moisture condition	$\sigma_3$ (kPa)	$E_0$ (kPa)	$E_{50}$ (kPa)	$\psi$ (°)
---	25	19942	12085	18.4
	50	40130	23409	17.6
	100	83454	47145	15.8
	200	186378	103729	15.4
---	25	23798	15109	16.0
	50	52648	29287	15.1
	100	110988	58079	14.6
---	25	11337	7551	16.8
	50	25633	15850	15.3
	100	47642	28714	14.9

### 3.1.3 Cable

Based on theoretical calculation for the predicted load capacity of block anchor, the cable used to pullout the block anchor was decided to be 5 mm diameter twisted steel cable. This cable has a breakout capacity of about 15.7 kN, at a maximum strain of about 3%. Additionally, the load-displacement behavior of the cable was obtained in terms of elongation ( $\Delta$ ) of cable vs. load level ( $P$ ). The length of cable tested was 80 cm, equals to that used for the pullout tests of block anchor. This is essential to correct the displacement of the block anchor for the elongation of the cable. Tests were performed according to ASTM Standard. The maximum applied load to the cable is 3.9 kN (400 kgf), which is more than the maximum load capacity for block anchors predicted from theoretical solutions.

The soil-cable interface friction was tested to determine friction resistance of a cable having the same length as the cable used for pullout tests of the block anchor. The pullout test was performed on the cable using similar apparatus and procedure for block anchor pullout tests. The cable was embedded in the sand box at a depth of 225mm (the same depth of the cable for the block anchor). Measurements indicated that the maximum friction was only 32 N corresponding at a displacement of 0.5 mm. This is only about 2.4 % of the load for block anchor, its effect on the pullout load is neglected.

### ***3.2 Model Preparation***

A 150X150X150mm concrete block was tested in the laboratory to determine the pullout capacity of a scale model block anchor in sand. For comparison purposes, a 150X150mm steel plate anchor was also tested. During casting of concrete block, a steel cable was connected to reinforcements embedded into the block. The cable was positioned in the location of the pulling load, as estimated by theoretical calculation,  $z = 80\text{mm}$ .

Tests were made in a box, which is 1200mm long, 800mm wide and 600mm high. The box walls are watertight plexi-glass and are stiffened by steel bracing to sustain soil pressure. At the bottom of the box, a network of perforated  $\frac{1}{2}$  in PVC pipes enclosed with geotextile was installed for supply and drainage of water to allow testing at various moisture conditions. The box was filled with sand by pluviation method by an automated sand-laying machine to produce uniformly dense, homogenous, isotropic and reproducible sand; deposited by free-falling dry sand from a height of fall of about 1m. The showering continues in lifts until the bottom 300mm of the box is filled with sand to the desired elevation. The block anchor, with the two pressure transducers attached at bottom and the plate mounted on the top, is placed on the deposited sand at a distance 800mm from the front wall of the sand box (passive side) and in the middle between the two sides of sand box. The cable is stretched to the loading device, hooked at the load cell. Then, sand deposition is resumed until the box is filled with sand.

To reconstitute the model for the next test, the measuring devices were disconnected, the soil was excavated carefully down to 100mm below the bottom of the block anchor, the anchor block is taken, then the model is rebuilt.

For testing at saturation condition, water was gradually supplied to the sand through network of pipes at the bottom of the box, until the water spills from the top of the box. The valve was closed and the sand was kept saturated, for pullout testing of anchor at saturation condition.

For testing at wet/unsaturated condition, the sand is first saturated, then water was drained out through the pipes at the bottom of the box until the water reaches the bottom 100mm. The valve was closed and the pullout testing of anchor was made while the sand is at wet/unsaturated condition. To assess moisture conditions, soil samples were taken from random positions at depths between 15 cm and 30 cm from the surface. The water content ( $w$ ) was found to be 12.5 %, which corresponds to a degree of saturation of 65.6%.

To measure the vertical pressure at the interface between soil and the bottom of the block anchor, two pressure transducers were used, one at the front-bottom and one at the back-bottom of the block anchor. The pressure transducers have diameter of 5 mm, maximum pressure of 200 psi.



Movements (vertical and horizontal) of the anchor placed inside the soil were monitored by four vertical and two horizontal LVDT's placed at an aluminum plate mounted on the block and extended above the surface. To minimize the earth pressure on this plate, its stem is oriented such that the 4mm thickness faces the direction of pulling.

### ***3.3 Pullout Testing***

Loading machine is mainly a gear box driven by fractional motor connected to screw-spindle to move backward (pulling motion) at a rate of 0.167 mm/min (1 cm/hour). A load cell was placed between cable and screw-spindle. The load cell is screwed to spindle screw. To connect cable to the load cell, a special high-strength hook was attached to the load cell. A load cell was used measure the pullout load generated by the loading machine. It is a medium range tension having maximum allowable capacity of 500 kgf. At the back of the gear box, a third horizontal LVDT was placed.

Load cell, LVDT's, and pressure transducer were calibrated before being used. Data logger was used to simultaneously record all ten measurements, consisting of one load cell, seven LVDT's (four vertical and three horizontal) and two pressure transducers. After each test, all data recorded were transferred to PC for post-processing.

Testing involves pulling the anchor until failure. Sets of pullout tests were made on block anchors at dry, wet and saturation conditions of sand. For comparison purposes, a set of pullout tests were made on plate anchors at dry sand condition. During testing, readings of various devices were monitored, and deformations of sand surface were visually observed, mapped (measurement of length, width and height were taken), and photographed. Failure conditions of the soil surface were observed at both the front of the anchor (passive side) and at the back of the anchor (active side).

## **4. RESULTS AND DISCUSSIONS**

The effect of moisture condition of sand is presented for dry, wet and saturated condition. Figure 3 shows typical the load-displacement relationship for block anchor embedded in sand at dry, wet and saturated conditions. The displacement represents the actual displacement of the block anchor, which was obtained after correcting the measured displacement by the horizontal LVDT at the end of the cable from cable elongation and other connection displacements.

For the dry condition, the values of the ultimate pullout load and the corresponding displacement are 1310 N and 16.71 mm, respectively. For the wet condition, the values of the ultimate pullout load and the corresponding displacement are 2298 N and 28.3 mm, respectively. For the saturated condition, the values of the ultimate pullout load and the corresponding displacement are 705 N and 21.07 mm,

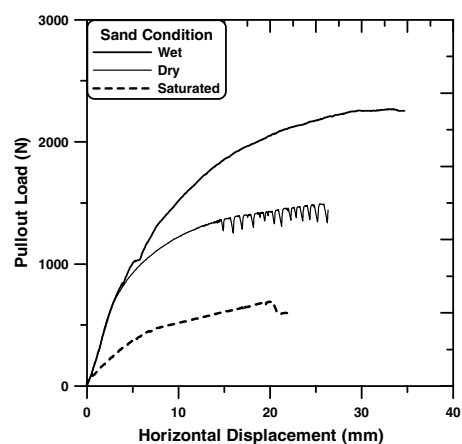
respectively. As a comparison, results from testing plate anchor in dry sand give the ultimate pullout load and the corresponding displacement to be 1200 N and 16.54 mm, respectively. It can be seen that the thickness of the block increases the ultimate load increases, due to the fact that the friction at the sides and top of the anchor contribute to the pullout capacity.

Figure 4 depicts the variation of the pullout loads versus moisture condition. It shows that the wet condition gives the highest pullout load, approximately 70 % higher than that for dry condition. This is due the increase of the bulk density and the present of apparent cohesion caused by the capillarity force. Saturated condition shows approximately 50 % reduction in pullout load compared to the dry condition, which is due to low effective unit weight.

The values of  $\delta_{\text{mobilized}}$  for Coulomb theory are  $11.2^\circ$ ,  $7.7^\circ$ , and  $11.4^\circ$  for dry, wet, and saturated conditions, respectively, for concrete block. The corresponding values for Log spiral theory are:  $10.9^\circ$ ,  $7.3^\circ$ , and  $11.0^\circ$ . For steel plate in dry sand, values of  $\delta_{\text{mobilized}}$  are  $2.2^\circ$ , and  $2.1^\circ$  for Coulomb and Log spiral theories, respectively.

The correction factor (M) to account for the 3-D effect, equation (2), is given in Table 2. Figure 5 presents results of the analytical solutions according to equation (3), with  $F_t = 0$  (as it was observed that the top soil moves with the block not relative to it).

The vertical displacements measured using four LVDT's indicate uplifting and tilting of the block anchor towards the passive side. Pressure transducers at the bottom of the anchor block indicate uplifting of the block, although the one at the passive side is highly contaminated by the vertical component of the passive pressure.



**Figure 3. Load-displacement curves for anchor block in sand of different moisture conditions.**

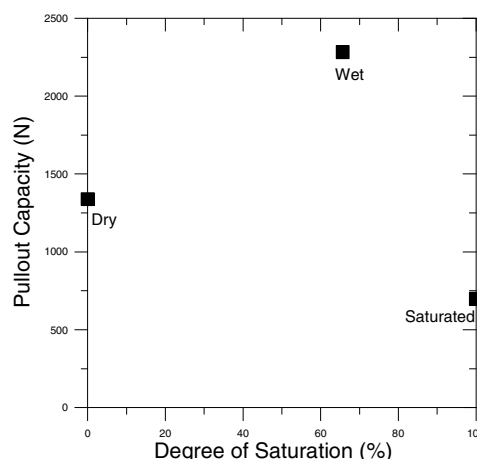


**Figure 4. Pullout capacity of anchor block vs. degree of saturation of sand**

**Table 2. The correction factor (M) for the 3-D effect**

Anchor type	Moisture condition	Theory		
		Rankine	Coulomb	Log Spiral
Block	Dry	2.76	4.26	4.39
	Wet	2.76	3.63	3.79
	Saturated	2.76	4.29	4.42
Plate	Dry	2.76	2.96	3.08

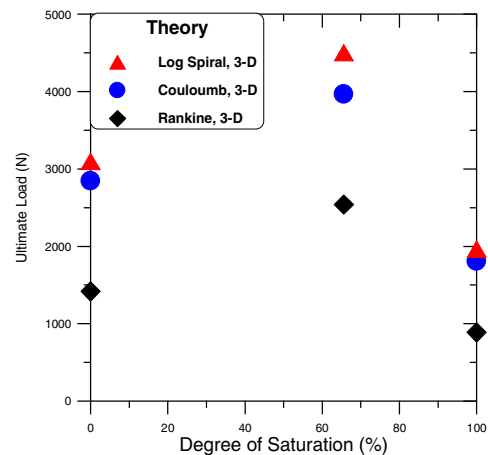


**Figure 5. Results of the analytical solutions.**

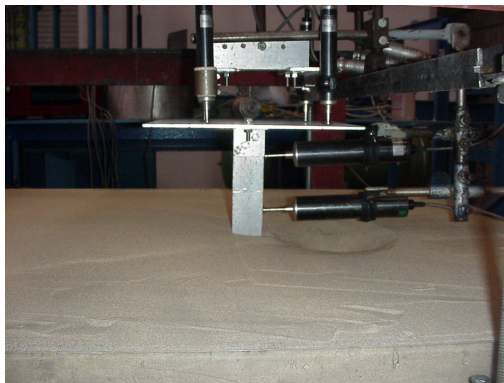
Typical failure conditions of the soil surface are presented in Figure 6 for dry and wet conditions. At the passive side, a bulging area was seen on the soil surface in front of the anchor for every test except for the wet condition. At the active side, an elliptic depression was found at the back of the anchor for dry condition. For saturated condition, a settlement of soil behind the anchor was observed. For wet/unsaturated condition, cracks were observed at both the passive side and the active side, with width varying between 1 and 5mm.

## 5. CONCLUSIONS

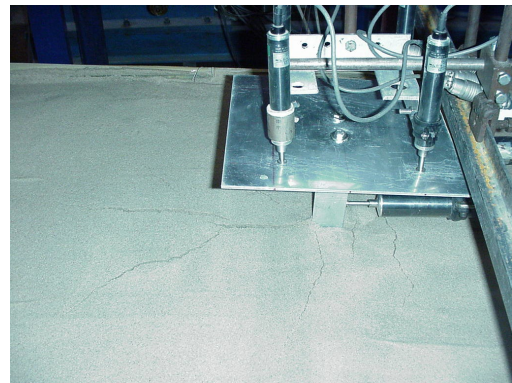
1. The moisture condition of the soil highly affects the pullout capacity of the block anchor. The wet condition gives the highest pullout capacity value, and the saturated condition gives the lowest.
2. Thickness of anchor contributes to the pullout capacity through friction forces. This contribution is not so significant as compared to the passive resistance.
3. Pullout capacity of block anchor by Rankine's theory, corrected for the 3-D effect with the frictions contributions, shows close agreement with experimental results.
4. The pressure below the block at the passive side is higher than that at the active side.
5. Vertical displacement indicated that there is an uplifting and tilting of the block
6. Horizontal displacements, needed to develop the maximum pullout capacity, were 16.71, 28.3, and 21.07 mm for dry, wet, and saturated conditions, respectively.
7. Failure manifested itself by a bulged area on the surface of the sand located at the passive side, and by a depression in the active side, for dry condition. For wet condition, cracks appeared at both passive and active sides.

## ACKNOWLEDGEMENT

The author acknowledges the support of King Fahd University of Petroleum & Minerals. Also, the help of Mr. Al Sidqi Hasan and Mr. Hasan Zakaria is appreciated.



(a) Dry



(b) Wet/Unsaturated

**Figure 6. Failure conditions of the soil surface.**

## REFERENCES

- Akinmusuru, J.O . (1978). "Horizontally Loaded Vertical Plate Anchors in Sand". *Journal of Geotechnical Engineering Division*, ASCE, Vol.104, pp. 283-286.
- Bowles, J. E. (1997). *Foundation Analysis and Design (5<sup>th</sup> ed.)*. New York: McGraw-Hill. 1175 p.
- Das, B.M. (1975). "Pullout Resitance of Vertical Anchors". *Journal of Geotechnical Engineering Division*, ASCE, vol. 101 (GT1), pp. 87-91.
- Das, B.M. (1995). *Principles of Foundation Engineering (3<sup>rd</sup> ed.)*. California: Brooks/Cole Publishing Company.
- Dickin, E.A., and Leung, C.F. (1983). "Centrifugal Model Tests on Vertical Anchor Plates". *J. of Geotechnical Engineering*, ASCE, Vol. 109 (12), pp. 1503-1525.
- Duncan, M., and Mokwa, R. (2001). "Passive Earth Pressures: Theories and Test". *J. of Geotech. and Geoenvironmental Eng.*, ASCE, Vol. 127 (4), pp. 248-257.
- Ghaly, A.M. (1997). "Load-Displacement Prediction for Horizontally Loaded Vertical Plates". *J. of Geotech. and Geoenvironmental Eng.*, ASCE, Vol. 123 (1), pp. 74-76.
- Hansen, J.B. (1966). "Resistance of Rectangular Anchor Slab". *Danish Geotechnical Institute*, Copenhagen, Vol. 21, pp. 12-13.
- Hueckel, S. (1957). "Model Tests on Anchoring Capacity of Vertical and Inclined Plates". *Proceedings of Fourth International Conference on Soil Mechanics and Foundation Engineering*, London, Vol. 2, pp. 203-206.
- Neeley, W.J., Stuart, J.G., Graham, J. (1973). "Failure Loads of Vertical Anchor Plates in Sands". *Journal of Soil Mechanics and Foundations Division*, Proceedings of ASCE, Vol. 99 (9), pp. 669-685.
- Ovesen, N.K. (1964). "Passive Anchor Slabs, Calculation Methods and Model Tests". *Danish Geotechnical Institute*, Bull. no. 4, pp. 5-39.
- Ovesen, N.K. and Stromann, H. (1972), "Design Methods for Vertical Anchor Slabs in Sand", Proceedings, Speciality Conference on Performance of Earth and earth-Supported Structures. ASCE, Vol. 2.1, pp.1481-1500.
- Singh, A.I. (1967). *Soil Engineering in Theory and Practice*. New York: Asia Publishing House, Inc.